

Maria Rosa González-Siso, Xavier Gaona*, Lara Duro, Marcus Altmaier and Jordi Bruno*

Thermodynamic model of Ni(II) solubility, hydrolysis and complex formation with ISA

DOI 10.1515/ract-2017-2762

Received January 13, 2017; accepted May 23, 2017; published online July 14, 2017

Abstract: The solubility of β -Ni(OH)₂(cr) was investigated at $T=(22\pm 2)^\circ\text{C}$ in the absence and presence of α -isosaccharinic acid (ISA), the main degradation product of cellulose under alkaline pH conditions. Batch solubility experiments were performed from undersaturation conditions under inert gas (Ar) atmosphere. Solubility experiments in the absence of ISA were conducted in 0.5 and 3.0 M NaCl–NaOH solutions at $7.5 \leq \text{pH}_m \leq 13$ (with $\text{pH}_m = -\log_{10}[\text{H}^+]$). XRD analyses of selected solid phases collected after completing the solubility experiments (≈ 300 days) confirmed that β -Ni(OH)₂(cr) remains as solid phase controlling the solubility of Ni(II) in all investigated conditions. Based on the slope analysis ($\log_{10}[\text{Ni}]$ vs. pH_m) of the solubility data and solid phase characterization, the equilibrium reactions β -Ni(OH)₂(cr) + 2 H⁺ \rightleftharpoons Ni²⁺ + 2 H₂O(l) and β -Ni(OH)₂(cr) \rightleftharpoons Ni(OH)₂(aq) were identified as controlling the solubility of Ni(II) within the investigated pH_m region. The conditional equilibrium constants determined from the solubility experiments at different ionic strengths were evaluated with the specific ion interaction theory (SIT). In contrast to the current thermodynamic selection in the NEA–TDB, solubility data collected in the present work does not support the formation of the anionic hydrolysis species Ni(OH)₃[−] up to $\text{pH}_m \leq 13.0$. Solubility experiments in the presence of ISA were conducted in 0.5 M NaCl–NaOH–NaISA solutions with $0.01 \text{ M} \leq [\text{NaISA}] \leq 0.2 \text{ M}$ and $9 \leq \text{pH}_m \leq 13$. XRD analyses confirmed that β -Ni(OH)₂(cr) is also the solid phase controlling the solubility of Ni(II) in the presence of ISA. Solubility data of all investigated systems can be properly

explained with chemical and thermodynamic models including the formation of the complexes NiOHISA(aq), Ni(OH)₂ISA[−] and Ni(OH)₃ISA^{2−}. The reported data confirm the low solubility ($<10^{-7}$ M) of Ni(II) in hyperalkaline pH conditions representative of cementitious environments ($10 \leq \text{pH} \leq 13$), which increases to up to 10^{-5} M in the presence of 0.2 M NaISA. These results significantly improve source term estimations for Ni(II) in environments relevant for the disposal of low and intermediate level radioactive waste (L/ILW). The chemical and thermodynamic models derived in this work can be implemented in geochemical models/calculations, and provide further confidence in the safety analysis of repositories for the disposal of L/ILW.

Keywords: Nickel(II), solubility, hydrolysis, ISA, thermodynamics, SIT.

1 Introduction

The Swedish Final Repository SFR1 at Forsmark started in 1988 to operate the final disposal of low- and intermediate level radioactive waste (L/ILW) in Sweden. Due to the predicted growth of L/ILW as a result of the planned dismantling and reactor licencing activities, SKB is planning the construction of an extension of SFR1 under the name of SFR3 (from here on we will unify them under the name of SFR). In both cases, cementitious materials play an important role, not only as an immobilization matrix for the waste itself but also as backfill and construction material for galleries and storage vaults. These materials will impose highly alkaline pH conditions ($10 \leq \text{pH} \leq 13.3$) on the intruding water over a very long time scale [1]. The resulting alkaline porewaters will have a strong impact on the solubility, hydrolysis and complexation reactions of the radionuclides disposed of in SFR.

⁵⁹Ni ($t_{1/2} = 7.5 \cdot 10^4$ a) and ⁶³Ni ($t_{1/2} = 96$ a) are activation products of stable isotopes of Ni, Zn and Co disposed of in SFR as a component in the spent ion-exchange resins resulting from the cleaning of the reactor coolant water [2]. According to the long-term safety analysis of SFR, both isotopes are important contributors to the radiotoxicity of the disposed wastes [3]. ⁵⁹Ni can be found in the austenitic

*Corresponding authors: **Xavier Gaona**, Institute for Nuclear Waste Disposal, Karlsruhe Institute of Technology, P.O. Box 3640, 76021 Karlsruhe, Germany, E-mail: xavier.gaona@kit.edu; and **Jordi Bruno**, Amphos²¹, Passeig Garcia i Faria, 49-51, 1-1a, 08019 Barcelona, Spain, E-mail: jordi.bruno@amphos21.com
Maria Rosa González-Siso and Lara Duro: Amphos²¹, Passeig Garcia i Faria, 49-51, 1-1a, 08019 Barcelona, Spain
Marcus Altmaier: Institute for Nuclear Waste Disposal, Karlsruhe Institute of Technology, P.O. Box 3640, 76021 Karlsruhe, Germany

steel in the reactor, as activation product of Ni dissolved in the coolant and in corrosion particles deposited on the core. In the case of ^{63}Ni , sources are austenitic steels in the core. Stainless steel contains around 10% of Ni, increasing further to 50–75% in Inconel. Furthermore, Ni is also found as an impurity in Zircaloy (approx. 40 ppm) and in reactor fuel (approx. 20 ppm) [2]. Using the estimated inventory of radionuclides expected in SFR1 repository and the volumes and amounts of cement in SFR1 [4, 5], Grivé et al. [6] concluded that the maximum concentration of Ni active isotopes, ^{59}Ni and ^{63}Ni expected in the different vaults is in the range of $2.5 \cdot 10^{-5} \text{ mol dm}^{-3}$ to $2.5 \cdot 10^{-7} \text{ mol dm}^{-3}$.

Low- and intermediate level radioactive waste contains both organic and inorganic ligands. The main sources of organic ligands present in SFR are decontamination agents at the nuclear power plant (EDTA, DTPA, NTA, among others), degradation products of bitumen, ion exchange resins, cellulose and cement additives. An accurate knowledge of radionuclide interaction with the remaining organic ligands is important because of the potential impact of complexation on radionuclide solubility and sorption. Under highly alkaline cement porewaters, cellulose is slowly degraded to low molecular weight compounds. The final products depend on the porewater composition, although the presence of Ca^{2+} favours the formation of α -isosaccharinic acid (ISA, see Figure 1) [7–11]. Hence, ISA is considered as one of the main representatives of polyhydroxy carboxylic acids expected in cementitious environments.

Within this framework, an accurate knowledge of the solution chemistry of Ni(II) under alkaline to hyperalkaline pH conditions and the impact of ISA on the solubility of Ni(II) in cementitious environments is very relevant to assess the source term (i.e. robust upper-limit values of the aqueous Ni(II) concentration in the direct vicinity of the waste packages) of Ni(II) in repositories for the disposal of L/ILW, and thus in the safety assessment of SFR.

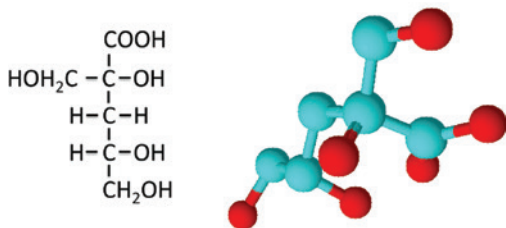


Figure 1: Two representations of the α -isosaccharinic acid (α -ISA) chemical structure.

2 Discussion of previous experimental studies in the literature

2.1 Solubility and hydrolysis of Ni(II) in the absence of ISA

The solution chemistry of Ni(II) is characterized by a moderate hydrolysis and the formation of the sparingly soluble oxo-hydroxides under alkaline to hyperalkaline pH conditions. Theophrastite ($\beta\text{-Ni}(\text{OH})_2(\text{cr})$) is the solid phase controlling the solubility of Ni(II) at $T=25^\circ\text{C}$, transforming into bunsenite ($\text{NiO}(\text{cr})$) above $T=77^\circ\text{C}$ [12]. Several experimental studies have previously investigated the solubility of $\beta\text{-Ni}(\text{OH})_2(\text{cr})$ in aqueous systems. These publications were critically reviewed in the NEA–TDB volume dedicated to Ni [13]. One of the relevant shortcomings identified in many of the reviewed solubility studies was the insufficient knowledge/characterization of the Ni solid phase controlling the solubility, especially in terms of crystallinity (e.g. particle size) and presence of impurities (e.g. Na^+ , Cl^-). The effect of particle size on the solubility constant of a solid is a well-known effect which is particularly critical for metal oxides [14–16]. This is also reflected in the large differences of $\log_{10} {}^*K_{s,0}^\circ\{\beta\text{-Ni}(\text{OH})_2(\text{cr})\}$ reported in the literature (see Table 1). Indeed, the recent review by Brown and Ekberg [18] classified the solubility data available for $\beta\text{-Ni}(\text{OH})_2(\text{cr})$ with respect to their crystallinity and proposed $\log_{10} {}^*K_{s,0}^\circ\{\beta\text{-Ni}(\text{OH})_2(\text{cr})\}=(11.75 \pm 0.13)$ for the microcrystalline phase and (10.96 ± 0.20) for the more crystalline one.

Several hydrolysis species of Ni(II) are selected in the NEA–TDB review, namely NiOH^+ , $\text{Ni}_2\text{OH}^{3+}$, $\text{Ni}_4(\text{OH})_4^{4+}$ and $\text{Ni}(\text{OH})_3^-$ (see Table 1). The consideration in the selected chemical model of $\text{Ni}(\text{OH})_3^-$ as the only species forming under alkaline to hyperalkaline conditions was based on a single solubility study at 25°C [20]. A very large uncertainty was assigned to the selected hydrolysis constant to reflect the outcome of additional experimental data gathered at higher temperatures [27, 28]. Solubility data reported in Gayer and Garret [20] was also re-interpreted within the ThermoChimie project including the predominance under alkaline to hyperalkaline pH conditions of both $\text{Ni}(\text{OH})_2(\text{aq})$ and $\text{Ni}(\text{OH})_3^-$ [17]. Conversely, more recent solubility studies with $\text{NiO}(\text{cr})$ and $\beta\text{-Ni}(\text{OH})_2(\text{cr})$ did not observe the formation of $\text{Ni}(\text{OH})_3^-$ up to $\text{pH}\approx 13$ [12, 26, 29, 30]. Instead, these authors proposed the only formation of Ni^{2+} and $\text{Ni}(\text{OH})_2(\text{aq})$ in the aqueous phase. Felipe–Sotelo et al. [31] found also a very low solubility

Table 1: Equilibrium constants available in the literature, selected in NEA–TDB [13], ThermoChimie [17] databases and the review by Brown and Ekberg [18] for the solubility and hydrolysis of Ni(II).

		References
Solubility	$\log_{10} {}^*K_{s,0}^{\circ}$	
$\beta\text{-Ni(OH)}_2(\text{cr}) + 2 \text{H}^+ \Leftrightarrow \text{Ni}^{2+} + 2 \text{H}_2\text{O}(\text{l})$	12.20 ^{a,b,c}	Britton [19]
	10.78 ^{b,d}	Gayer and Garrett [20]
	10.80 ^{b,d}	Feitknecht and Hartmann [21]
	10.89 ^{b,d}	Novak-Adamic et al. [22]
	12.1	Poulson and Drever [23]
	(11.9 ± 0.1)	Mattigod et al. [24]
	(10.52 ± 0.59)	Plyasunova et al. [25] – review
	11.81 ^c	Ziemniak and Goyette [26]
	(11.03 ± 0.28)	Gamsjäger et al. [13] – review
	(11.67 ± 0.20) ^c	Palmer and Gamsjäger [12]
	(11.03 ± 0.28)	Giffaut et al. [17] – review
	(10.96 ± 0.20) ^d	Brown and Ekberg [18] – review
	(11.75 ± 0.13) ^c	Brown and Ekberg [18] – review
Hydroxide complexes	$\log_{10} {}^*K_{(1,n)}^{\circ}$	
$\text{Ni}^{2+} + \text{H}_2\text{O}(\text{l}) \Leftrightarrow \text{NiOH}^+ + \text{H}^+$	–(9.54 ± 0.14)	Gamsjäger et al. [13] – review
	–(9.54 ± 0.14)	Giffaut et al. [17] – review
	–(9.90 ± 0.03)	Brown and Ekberg [18] – review
$2 \text{Ni}^{2+} + \text{H}_2\text{O}(\text{l}) \Leftrightarrow \text{Ni}_2\text{OH}^{3+} + \text{H}^+$	–(10.6 ± 1.0) ^e	Gamsjäger et al. [13] – review
$4 \text{Ni}^{2+} + 4 \text{H}_2\text{O}(\text{l}) \Leftrightarrow \text{Ni}_4(\text{OH})_4^{4+} + 4 \text{H}^+$	–(27.52 ± 0.15)	Gamsjäger et al. [13] – review
	–(27.52 ± 0.15)	Giffaut et al. [17] – review
	–(27.9 ± 0.6)	Brown and Ekberg [18] – review
$\text{Ni}^{2+} + 2 \text{H}_2\text{O}(\text{l}) \Leftrightarrow \text{Ni(OH)}_2(\text{aq}) + 2 \text{H}^+$	–(18.0 ± 0.3)	Giffaut et al. [17] – review
	–(21.15 ± 0.06)	Brown and Ekberg [18] – review
$\text{Ni}^{2+} + 3 \text{H}_2\text{O}(\text{l}) \Leftrightarrow \text{Ni(OH)}_3^- + 3 \text{H}^+$	–(29.2 ± 1.7)	Gamsjäger et al. [13] – review
	–(29.2 ± 1.7)	Giffaut et al. [17] – review

^a $T=18^\circ\text{C}$; ^bAs calculated by Gamsjäger et al. [13]; ^cClassified as micro-crystalline $\beta\text{-Ni(OH)}_2(\text{cr})$ in Brown and Ekberg [18]; ^dClassified as crystalline $\beta\text{-Ni(OH)}_2(\text{cr})$ in Brown and Ekberg [18]; ^eSame stability constants recommended in Giffaut et al. [17] and Brown and Ekberg [18]. All data reported at $T=25^\circ\text{C}$, except otherwise indicated.

of Ni(II) in 0.02 M NaOH ($\approx 5 \cdot 10^{-8}$ M). This observation is again not consistent with the formation of a very stable Ni(OH)_3^- species. The very discrepant results available in the literature are possibly related with the very strong Ni(II)–carbonate complexation ($\log_{10} \beta_{11}^{\circ} = (4.2 \pm 0.4)$ for $\text{Ni}^{2+} + \text{CO}_3^{2-} \Leftrightarrow \text{NiCO}_3(\text{aq})$, as selected in [13]), which requires that solubility experiments in the alkaline pH range are performed in inert-gas atmosphere under strict exclusion of CO_2 . The uncertainties affecting the thermodynamically calculated solubility and hydrolysis of Ni(II) under alkaline to hyperalkaline conditions represent an important limitation when assessing the chemical behaviour of this radionuclide in cementitious systems, and deserves further experimental studies.

2.2 Complexation of Ni(II) with ISA

Only a very limited number of experimental studies are available in the literature dedicated to the complexation

of Ni(II) with ISA [25, 31–34].¹ From these studies, only Warwick et al. [32] and Almond et al. [33] provide thermodynamic data for Ni(II)–ISA aqueous complexes forming under the alkaline to hyperalkaline pH conditions relevant in cementitious systems (see Table 2). Both studies combined analogous experimental techniques (spectrophotometry and potentiometric titrations) and used very high Ni(II) concentrations (up to 0.01 M) for the determination of the stoichiometry of the complexes forming. Note that under hyperalkaline pH conditions, these concentrations of Ni(II) are clearly above the solubility limit of $\beta\text{-Ni(OH)}_2(\text{cr})$ (both crystalline and micro-crystalline phases, see Section 2.1). Warwick et al. [32] and Almond et al. [33] conducted additional sorption experiments at lower $[\text{Ni(II)}]$ to determine the stability constants of the Ni(II)–ISA complexes according with

¹ All data in the peer-review paper by Warwick et al. [32] were originally reported in the PhD thesis by Evans [35].

Table 2: Equilibrium constants available in the literature for the complexation of Ni(II) with ISA.

Equilibrium reaction	pH	$\log_{10}K$	References
$\text{Ni}^{2+} + \text{ISA}^- \leftrightarrow \text{NiISA}^+$	6.2	1.99	Motellier and Charles [34]
	7.0	$(2.20 \pm 0.36)^a$	Warwick et al. [32]
	7.0	$(2.58 \pm 0.07)^b$	Warwick et al. [32]
	7.0	$(2.07 \pm 0.13)^c$	Almond et al. [33]
	7.0	$(1.94 \pm 0.15)^d$	Almond et al. [33]
$2\text{Ni}^{2+} + \text{ISA}^- + 4\text{OH}^- \leftrightarrow \text{Ni}_2(\text{OH})_4\text{ISA}^-$	13.0 ^e	(29.85 ± 0.89)	Warwick et al. [32]
	13.0 ^e	$(29.0 \pm 0.5)^c$	Almond et al. [33]
	13.0 ^e	$(30.6 \pm 0.5)^d$	Almond et al. [33]

^aDetermined by sorption (Schubert method); ^bDetermined by polarography; ^cCorresponding to the complexation with α -ISA; ^dCorresponding to the complexation with β -ISA; ^epH used for the quantification of the stability constants (Schubert method). Other pH values were used for the determination of the stoichiometry of the complexes. All data reported at $T = 25^\circ\text{C}$, except otherwise indicated.

the stoichiometry derived from spectroscopic/potentiometric measurements. Both Warwick et al. [32] and Almond et al. [33] proposed the formation of the aqueous species NiISA^+ and $\text{Ni}_2(\text{OH})_4\text{ISA}^-$ prevailing at $\text{pH} \approx 7$ and $\text{pH} \approx 13$, respectively. Although insufficiently characterized in the original publications, these studies reported also the formation of the solid $\text{Ni}_2(\text{OH})_3\text{ISA}(\text{s})$ at $7.2 < \text{pH} < 9.6$. Felipe-Sotelo et al. [31] investigated the solubility of Ni(II) in the absence and presence of cellulose degradation products (CDP), a complex mixture of polyhydroxycarboxylic compounds. The authors observed a clear increase in the solubility of Ni(II) at $\text{pH} \approx 12 - 13$ in the presence of CDP, although no quantitative interpretation was provided due to the intrinsic chemical complexity of their system.

Experimental data reported in Warwick et al. [32] were re-interpreted by Grivé et al. [6]. The latter authors argued that although polynuclear species may explain the data obtained at high $[\text{Ni}(\text{II})]$ (in spectrophotometric and potentiometric titrations), the formation of these species is very unlikely at the low $[\text{Ni}(\text{II})]$ used in the sorption experiments ($\approx 10^{-9}$ M). Instead, Grivé et al. [6] were able to properly explain sorption data by only defining the monomeric species NiISA^+ and $\text{Ni}(\text{OH})_3\text{ISA}^{2-}$. Note however that sorption experiments were only performed at $\text{pH} = 13$, and thus a conclusive experimental evidence of the stoichiometry of the Ni(II)–OH–ISA complex/es prevailing in this pH-region at low $[\text{Ni}(\text{II})]$ cannot be attained from these data only. These uncertainties represent a relevant limitation in the assessment of the chemical behaviour of Ni(II) in cementitious systems in the presence of cellulose degradation products.

3 Experimental description

3.1 Chemicals

All solutions were prepared with purified water (Milli-Q academic, Millipore) and purged for 2 h with Ar before use to remove traces of O_2 and CO_2 . All samples were prepared, stored and handled inside an inert gas (Ar) glovebox ($\text{O}_2 < 5$ ppm) at $T = (22 \pm 2)^\circ\text{C}$. A commercial $\text{Ni}(\text{OH})_2(\text{s})$ (Acros Organics) was used as solubility-controlling phase in all experiments. NaCl, NaNO_3 and $\text{Ca}(\text{OH})_2(\text{s})$ (all of them p.a.) were obtained from Merck. HCl and NaOH Titrisol® (Merck) were used to adjust the pH in the sample preparation. Carbonate impurities in 1.0 M NaOH (Titrisol) were quantified as $(3.1 \pm 0.2) \cdot 10^{-5}$ M.

NaISA(s) was synthesized in the present study from the alkaline degradation of α -lactose hydrate (Sigma Aldrich) following the approach summarized in Section 3.2. A Chelex® 100 ion exchange resin (Na-form, analytical grade, Sigma-Aldrich) was used for the conversion of $\text{Ca}(\text{ISA})_2(\text{s})$ into NaISA. Diethyl ether ($\text{C}_4\text{H}_{10}\text{O}$, ACS reagent grade, VWR BDH Prolabo®) was used to remove water from the final product.

3.2 Synthesis and characterization of NaISA(s)

The calcium salt of isosaccharinic acid was synthesized following the procedure reported by Whistler and BeMiller [36] with some modifications from Vercammen [37] and Evans [35]. In a first step, α -lactose hydrate was contacted with an aqueous solution saturated with $\text{Ca}(\text{OH})_2(\text{s})$, and the mixture stirred during 3 days at room temperature in an inert gas (Ar) glovebox. The resulting suspension was heated for 10 h and filtered whilst hot. A final volume reduction was performed in a rotary evaporator, and the mixture was left overnight at $T = 9^\circ\text{C}$. The resulting white crystals ($\text{Ca}(\text{ISA})_2(\text{s})$) were removed by filtration and washed with cold water, ethanol and acetone.

$\text{Ca}(\text{ISA})_2(\text{s})$ was converted into NaISA(s) using a cation exchange resin in the Na-form. An accurate description of the method is reported by Greenfield et al. [38], Glaus et al. [39], Pointeau et al. [40], Colàs [41], among others. Briefly, 2 g of $\text{Ca}(\text{ISA})_2(\text{s})$ were suspended in 500 mL of Milli-Q water in the presence of 25 g of resin. The mixture was agitated with a magnetic stirrer for approximately 1 h, and then filtered with filter paper (Whatman blue ribbon, $< 2 \mu\text{m}$). The filtrate was evaporated on a heating plate at

$T=60^{\circ}\text{C}$ until a brown viscous liquid was obtained. The remaining water content was removed using water-free diethyl-ether. The combination of repeated addition/evaporation of diethyl ether with a cooling step ($T=9^{\circ}\text{C}$, laboratory fridge) resulted in a pale yellow solid phase, NaISA(s).

Both $\text{Ca}(\text{ISA})_2(\text{s})$ and NaISA(s) were characterized using XRD (X-ray diffraction), (solution) ^1H and ^{13}C NMR (nuclear magnetic resonance), quantitative chemical analysis and TOC (total organic content). XRD measurements were performed using a D8 Advance diffractometer (Bruker AXS) equipped with a Cu radiation tube. The resulting diffractograms were compared with data reported in the literature for $\text{Ca}(\text{ISA})_2(\text{cr})$, and confirmed the only presence of the Ca-salt of ISA [42]. Appropriate amounts of $\text{Ca}(\text{ISA})_2(\text{s})$ and NaISA(s) were dissolved in weakly alkaline solutions ($\text{pH}\approx 9$) and the resulting solutions characterized using ^1H and ^{13}C NMR. NMR spectra of these samples were recorded at $T=300\text{ K}$ on a Bruker Avance III 400 spectrometer. The results confirm that ISA is the main organic component in both $\text{Ca}(\text{ISA})_2(\text{s})$ and NaISA(s) (>95%).

Ratios of Ca:ISA and Na:ISA in $\text{Ca}(\text{ISA})_2(\text{s})$ and NaISA(s) synthesized in the present work were quantified by a combination of quantitative chemical analysis and TOC measurements. Appropriate amounts of both solid phases were dissolved in water, and [Na] and [Ca] were quantified by ICP-OES (Optima 8300 DV, Perkin Elmer) and ICP-MS (X-Series II, Thermo Scientific), respectively. Aliquots of the same samples were also investigated by TOC using a Shimadzu TOC5000 equipment. The combination of these data resulted in Ca:ISA and Na:ISA ratios of 1:2 and 1:1, respectively, confirming the successful synthesis of the targeted $\text{Ca}(\text{ISA})_2(\text{s})$ and NaISA(s) compounds.

3.3 pH Measurements

A combination glass pH electrode (type ROSS, Orion), freshly calibrated against dilute standard pH buffers (pH 7–13, Merck), was used to determine the molal H^+ concentration, $[\text{H}^+]$ (with $\text{pH}_m = -\log_{10}[\text{H}^+]$). The experimentally measured pH values (pH_{exp}) are related to $[\text{H}^+]$ by $\text{pH}_m = \text{pH}_{\text{exp}} + A_m$, where A_m is given as a function of background electrolyte concentration. A_m -factors used in this work for NaCl and NaNO_3 were taken from Altmaier et al. [43] and Herm et al. [44], respectively. In NaCl–NaOH solutions with $[\text{OH}^-] > 0.03\text{ M}$, the H^+ concentration was calculated from the given $[\text{OH}^-]$ and the conditional ion product of water.

3.4 Solubility measurements with $\text{Ni}(\text{OH})_2(\text{s})$ in the absence and presence of NaISA

Batch solubility experiments in the absence of ISA were performed from undersaturation conditions with a commercially obtained $\text{Ni}(\text{OH})_2(\text{s})$. A total of 32 independent batch samples were prepared using 20 mg of $\text{Ni}(\text{OH})_2(\text{s})$ in 20 mL per experiment. Experiments were performed at constant ionic strength in 0.5 and 3.0 M NaCl–NaOH solutions with $7.5 \leq \text{pH}_m \leq 13$. One additional solubility sample was prepared in 0.5 M NaNO_3 with $\text{pH}_m \approx 9.3$ to assess the possible role of Ni(II)–Cl aqueous complexes in 0.5 M NaCl systems. [Ni] and pH_m were monitored at regular time intervals for up to 310 days. Dissolved [Ni] was measured after 10 kD ultrafiltration by ICP-MS (Thermo X-Series II). The detection limit of ICP-MS for Ni in 0.5 and 3.0 M NaCl–NaOH solutions was determined as $\log_{10}[\text{Ni}] \approx -7.9$ and -7.0 , respectively (3σ of repeated blank measurements). Experimental molar concentrations of Ni (M, $\text{mol}\cdot\text{L}^{-1}$) determined by ICP-MS were transformed to molal units (m, $\text{mol}\cdot\text{kg}^{-1}\text{ H}_2\text{O}$) using the conversion factors reported in Guillaumont et al. [45].

Ni(II) solubility experiments in the presence of NaISA were conducted using the same solid phase and experimental approach as in the absence of NaISA. A total of 28 independent batch samples were prepared in 0.5 M NaCl–NaOH–NaISA solutions with $0.01\text{ M} \leq [\text{ISA}^-] \leq 0.2\text{ M}$ and $9 \leq \text{pH}_m \leq 13$. [Ni] and pH_m were monitored at regular time intervals for up to 290 days.

The original $\text{Ni}(\text{OH})_2(\text{s})$ solid phase material was characterized before the start of the solubility experiments by XRD using a Bruker D8 Advance diffractometer (Cu $K\alpha$ radiation) equipped with a Sol-X detector. For this purpose, a small amount (1–2 mg) of the original solid phase pre-equilibrated in a 0.1 M NaCl solution with $\text{pH}_m \approx 11$ was washed 3 times with ethanol (2 mL) under Ar-atmosphere to remove the matrix solution. After the last cleaning step, the solid was suspended in approximately 20 μL ethanol, transferred to a capped silicon single crystal sample holder (Dome, Bruker), dried in the Ar-box under protective atmosphere for a few minutes before sealing of the sample holder, and transferred outside the glovebox for the collection the XRD diffractogram. XRD data were collected within $8^{\circ} \leq 2\Theta \leq 80^{\circ}$, with a step size of 0.04° and 6 s accumulation time per step. Solid phase from selected solubility experiments in the absence and presence of NaISA were characterized after attaining equilibrium conditions (constant [Ni] and pH_m) following the same approach, and the collected diffractograms were compared with the XRD of the original $\text{Ni}(\text{OH})_2(\text{s})$ material with the aim of evaluating the

possible alteration of the solid phase in the course of the solubility experiments.

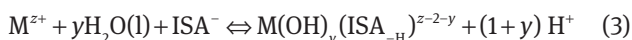
3.5 Development of chemical, thermodynamic and activity models

The development of a correct chemical model (set of equilibrium reactions defining the solution chemistry of a given system) for the behaviour of Ni(II) in alkaline to hyperalkaline pH conditions is based upon solid phase characterization and slope analysis of the solubility curves ($\log_{10}[\text{Ni}]$ vs. $\log_{10}[\text{H}^+]$ and $\log_{10}[\text{Ni}]$ vs. $\log_{10}[\text{ISA}]$), taking also into account previously reported chemical models for Ni(II) both in the absence and presence of ISA. This step sets the basis for the subsequent evaluation of thermodynamic and activity model parameters. The specific ion interaction theory (SIT) has been adopted in the present work to account for ion interaction processes and ionic strength effects [46], in agreement with the approach adopted within the NEA–TDB reviews [13, 45]. Within the SIT formalism, activity coefficients γ_j are calculated according with:

$$\log_{10}\gamma_j = -z_j^2 D + \sum_k \epsilon(j, k, I_m) m_k \quad (1)$$

where D is the Debye–Hückel term, z_j the charge of an ion j , I_m the molal ionic strength, m_k the molality of all ions k present in solution and $\epsilon(j, k, I_m)$ the specific ion interaction parameter. Experimental solubility data and thermodynamic models derived in the present work in the absence and presence of ISA are systematically compared with thermodynamic calculations using NEA–TDB [13] and ThermoChimie [17] databases, as well as with the recent review by Brown and Ekberg [18]. These are clearly the most comprehensive and up-to-date thermodynamic data selections for the systems investigated in the present work.

One of the main uncertainties still affecting the complexation of (hard) metal cations with ISA (or other polyhydroxycarboxylates in general) is the possible role of the alcohol groups in the chelation of the M^{z+} cation. Consequently, in experimental studies conducted under alkaline to hyperalkaline pH conditions, the release of protons eventually involved in the complexation reaction can be attributed to both hydrolysis of the M^{z+} cation or deprotonation of the α -hydroxyl group of ISA:



where $x=1+y$, and $\text{ISA}_{-\text{H}}^{z-2}$ corresponds to an ISA ligand with deprotonated carboxylic and α -hydroxyl groups. The type of complex forming has no impact on the mass-action law (except for the number of water molecules involved in the reaction), and thus does not affect the accordingly derived equilibrium constant/s for systems at low or intermediate ionic strength where the influence of the water activity is negligible. For the sake of simplicity, the quotation $\text{M}(\text{OH})_x \text{ISA}^{z-1-x}$ has been formally preferred in the present work. This must not be taken as a definitive indication of the type of complex forming. A detailed and conclusive proof-of-concept is thus still missing, but this aspect was not targeted within the work presented in this study.

Like other polyhydroxycarboxylic acids such as gluconic acid (GLU), ISA undergoes dehydration in acidic conditions to form a lactone L ($\text{HISA} \Leftrightarrow \text{L} + \text{H}_2\text{O}(\text{l})$) [47]. Because the formation of a lactone involves the reorganization of the ISA molecule, lactonization is a much slower process compared to the deprotonation reaction. Lactone formation has no relevance in the alkaline conditions investigated in this study, and thus has been disregarded in the thermodynamic interpretation of the Ni(II)–ISA system.

4 Experimental results in the absence of ISA

4.1 Solubility of Ni(II) in NaCl and NaNO₃ systems

Ni(II) experimental solubility data determined in the present work in NaCl–NaOH and NaNO₃ solutions in the absence of ISA are shown in Figure 2. Only values of $\log_{10}[\text{Ni}]$ quantified above the detection limit of ICP–MS for the given salt concentration are provided in the Figure. Note that in 3.0 M NaCl systems with $\text{pH}_m \geq 10.5$, all values of $\log_{10}[\text{Ni}]$ fell below the calculated detection limit and thus have been omitted. Solid lines in Figure 2 correspond to the solubility of β -Ni(OH)₂(cr) calculated using thermodynamic data derived in the present work (see Section 4.3), selected in NEA–TDB [13], ThermoChimie [17] and reported in the review by Brown and Ekberg [18] for a microcrystalline phase.

Constant pH_m and $\log_{10}[\text{Ni}]$ readings confirm that 310 days is sufficient contact time to attain thermodynamic equilibrium in all the investigated NaCl–NaOH and NaNO₃ systems. Two main regions can be identified in the experimentally determined solubility data:

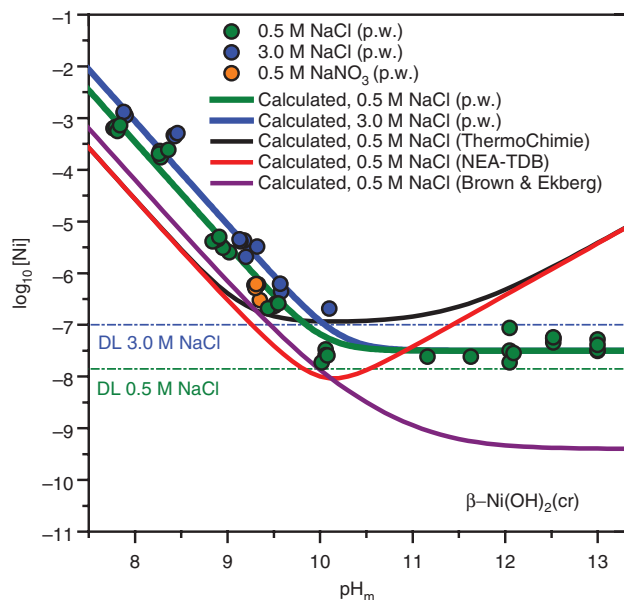


Figure 2: Ni(II) experimental solubility data determined in the present work in 0.5 M NaCl–NaOH, 0.5 M NaNO₃ and 3.0 M NaCl–NaOH. Solid lines corresponding to the solubility of β -Ni(OH)₂(cr) calculated according with the thermodynamic model derived in the present work (green line: 0.5 M NaCl; blue line: 3.0 M NaCl), selected in NEA–TDB [13] (red line), ThermoChimie [17] (black line) and in Brown and Ekberg [18] (purple line).

- **pH_m ≤ 10:** A steep decrease of the solubility with a well-defined slope of -2 ($\log_{10}[\text{Ni}]$ vs. pH_m) is observed in this pH-region for both 0.5 M and 3.0 M NaCl systems, indicating that two H⁺ are taken up in the equilibrium reaction controlling the solubility of Ni(II). Solubility data in 0.5 M NaNO₃ agree very well with solubility data in 0.5 M NaCl, indicating that both chloride and nitrate have a similar impact on the solubility of Ni(II) in this pH_m-region. Note further that the very small stability constants selected in the NEA–TDB for NiCl⁺ ($\log_{10}K_{11}^\circ = 0.08 \pm 0.6$) and NiNO₃⁺ ($\log_{10}K_{11}^\circ = 0.5 \pm 1.0$) complexes suggest that their contribution to the overall Ni(II) solubility is very minor for this background electrolyte concentration. Thermodynamic calculations using NEA–TDB, ThermoChimie or the selection in Brown and Ekberg [18] clearly underestimate experimental solubility determined in the present work, very likely due to differences in crystallinity (e.g. particle size) of the solid phase (see also discussion in Section 4.3).
- **pH_m ≥ 10:** Solubility data in 0.5 M NaCl–NaOH show a pH_m-independent trend up to pH_m ≈ 13, thus confirming that no H⁺ are involved in the equilibrium reaction controlling the solubility of Ni(II) in this pH_m-range. These experimental observations are in disagreement

with the increase in solubility calculated for this pH_m-region using thermodynamic data in NEA–TDB [13] and ThermoChimie [17], due to the selection of the anionic hydrolysis species Ni(OH)₃⁻ in both databases. On the contrary, our experimental observations are in line with NiO(cr) and β -Ni(OH)₂(cr) solubility data reported by Palmer and co-workers [12, 29, 30] (see Section 2.1). A good agreement is also obtained with recent Ni(II) solubility data in 0.02 M NaOH solutions, approached from both under- and oversaturation conditions [31]. Note however that, although the trend in our solubility data is in agreement with thermodynamic calculations using the selection in Brown and Ekberg [18], this model predicts a far too low solubility in this pH_m-region compared to our observations. A detailed discussion on this discrepancy is provided in Section 4.3.

4.2 Solid phase characterization

XRD analyses of the solid phase used in the present study confirm the only presence of Ni(OH)₂(s) as a solid phase controlling the solubility of Ni(II) (Figure 3). XRD patterns before and after solubility experiments are identical, and show a good match with the reference spectra of β -Ni(OH)₂(cr) (PDF 73-1520). Reflections of NaCl can be also observed in the solid phases recovered from solubility experiments in 3.0 M NaCl. This results from the insufficient removal of adhering matrix solution in concentrated NaCl solutions. In spite of this, XRD patterns corresponding to β -Ni(OH)₂(cr) can be unequivocally identified for these systems. Note that XRD patterns collected in the present work are virtually the same as those reported in Palmer and Gamsjäger [12] for β -Ni(OH)₂(cr), although notably narrower peak widths were observed by the latter authors. This observation indicates a more crystalline material than the one used in the present work.

4.3 Thermodynamic interpretation of Ni(II) solubility in the absence of ISA

Solid phase characterization by XRD in combination with slope analyses of experimental solubility data are used to derive the chemical reactions (4) and (5) as controlling the solubility of Ni(II) at $8 \leq \text{pH}_m \leq 13$. One of the critical issues discussed by Gamsjäger et al. [13] on the solubility of Ni(II) is the possible presence of basic salts contaminating β -Ni(OH)₂(cr), and the adverse impact on the determination of accurate thermodynamic functions of the latter solid. The satisfactory match of our solid phase with XRD

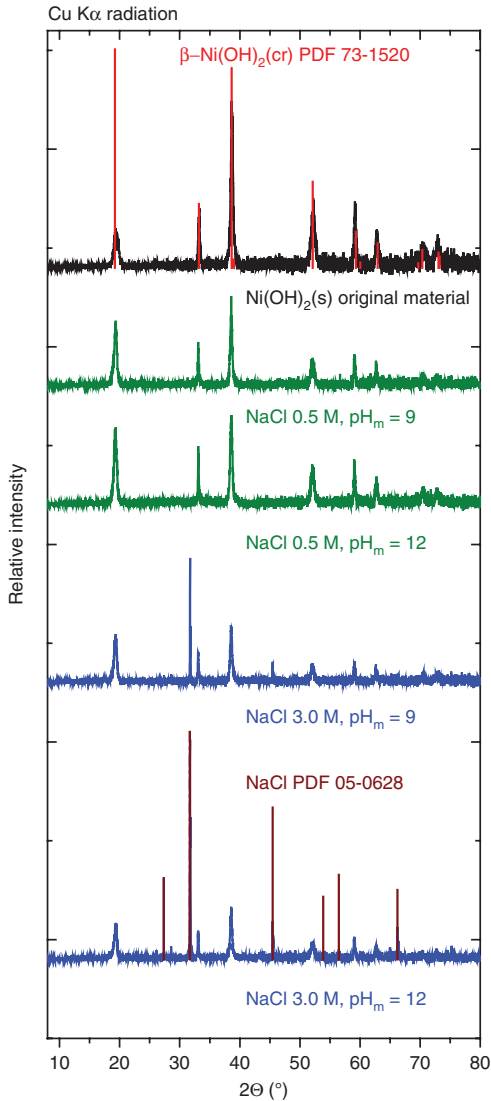
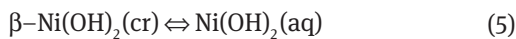
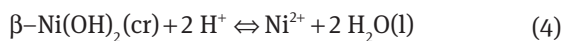


Figure 3: XRD spectra of selected solid phases from Ni(II) solubility experiments in 0.5 and 3.0 M NaCl. Red and brown marks indicate peak positions for β -Ni(OH)₂(cr) and NaCl reference spectra (PDF 73-1520 and PDF 05-0628, respectively).

patterns of β -Ni(OH)₂(cr) and the well-defined slope of -2 determined for the solubility data within $8 \leq \text{pH}_m \leq 9.5$ indicates that it is possible to disregard the presence of $\text{Na}_x\text{Ni}(\text{OH})_{2+x}(\text{s})$ or $\text{Ni}(\text{OH})_{2-x}\text{Cl}_x(\text{s})$ in the investigated solubility systems. The chemical model can be thus explained by using the equilibrium reactions:



With

$$\log_{10} {}^*K'_{s,0} = \log_{10} [\text{Ni}^{2+}] - 2 \log_{10} [\text{H}^+] \quad (6)$$

$$\log_{10} K'_{s,(1,2)} = \log_{10} [\text{Ni}(\text{OH})_2(\text{aq})] \quad (7)$$

and

$$\log_{10} {}^*K_{s,0}^\circ = \log_{10} {}^*K'_{s,0} + \log_{10} \gamma_{\text{Ni}^{2+}} - 2 \log_{10} \gamma_{\text{H}^+} + 2 \log_{10} a_w \quad (8)$$

$$\log_{10} K_{s,(1,2)}^\circ = \log_{10} K'_{s,(1,2)} \quad (9)$$

Based on the proposed chemical model, conditional solubility constants for the chemical reaction (4) were determined from experimental solubility data in 0.5 M and 3.0 M NaCl with $8 \leq \text{pH}_m \leq 9.5$ according with equations (6) and (7). Note however, that in this pH_m -region the formation of NiCl^+ is also predicted for 0.5 and 3.0 M NaCl solutions. In order to account for the contribution of NiCl^+ to $[\text{Ni}]_{\text{tot}}$, the stability constant reported for reaction (10) in Gamsjäger et al. [13] was recalculated to $I=0.5$ and 3.0 M NaCl by SIT, and $[\text{NiCl}^+]$ calculated accordingly. No selection of $\varepsilon(\text{NiCl}^+, \text{Cl}^-)$ was provided by Gamsjäger et al. [13], and thus this interaction coefficient was estimated in the present work from $\varepsilon(\text{NiCl}^+, \text{ClO}_4^-)$ based on the correlation between Cl^- and ClO_4^- coefficients described in Guillaumont et al. [45].



$$\log_{10} \beta_{1,1}^\circ = (0.08 \pm 0.60) \text{ [Gamsjäger et al. [13]]}$$

with

$$\varepsilon(\text{Ni}^{2+}, \text{Cl}^-) = (0.17 \pm 0.02) \text{ kg} \cdot \text{mol}^{-1} \text{ [Gamsjäger et al. [13]]}$$

and

$$\varepsilon(\text{NiCl}^+, \text{ClO}_4^-) = (0.47 \pm 0.06) \text{ kg} \cdot \text{mol}^{-1} \text{ [Gamsjäger et al. [13]]}$$

et al. [13]]

$$\varepsilon(\text{NiCl}^+, \text{Cl}^-) = 0.028 + 0.38 \varepsilon(\text{NiCl}^+, \text{ClO}_4^-) = (0.21 \pm 0.06) \text{ kg} \cdot \text{mol}^{-1} \text{ [estimated in p.w.]}$$

The SIT-plot resulting from the values of $\log_{10} {}^*K'_{s,0}$ ($I=0.5$ M NaCl) and $\log_{10} {}^*K'_{s,0}$ ($I=3.0$ M NaCl) is shown in Figure 4. Uncertainties of $\log_{10} {}^*K_{s,0}^\circ$ (intercept) and $-\Delta\varepsilon$ (slope) are calculated following the NEA guidelines for the estimation of errors [48], which accounts also for the uncertainties of the experimental errors in $\log_{10} {}^*K'_{s,0}$.

The slope of the SIT-plot corresponds to $-\Delta\varepsilon = -(\varepsilon(\text{Ni}^{2+}, \text{Cl}^-) - 2\varepsilon(\text{H}^+, \text{Cl}^-)) = (0.01 \pm 0.05) \text{ kg} \cdot \text{mol}^{-1}$. Considering $\varepsilon(\text{H}^+, \text{Cl}^-) = (0.12 \pm 0.01) \text{ kg} \cdot \text{mol}^{-1}$ as reported in Gamsjäger et al. [13], the value $\varepsilon(\text{Ni}^{2+}, \text{Cl}^-) = (0.25 \pm 0.05) \text{ kg} \cdot \text{mol}^{-1}$ can be calculated. This result is in moderate agreement with the value currently selected in Gamsjäger et al. [13] (0.17 ± 0.02).

The solubility product determined in the present work for β -Ni(OH)₂(cr) ($\log_{10} {}^*K_{s,0}^\circ = 12.10 \pm 0.11$) is clearly larger than the value selected in the NEA-TDB [13]

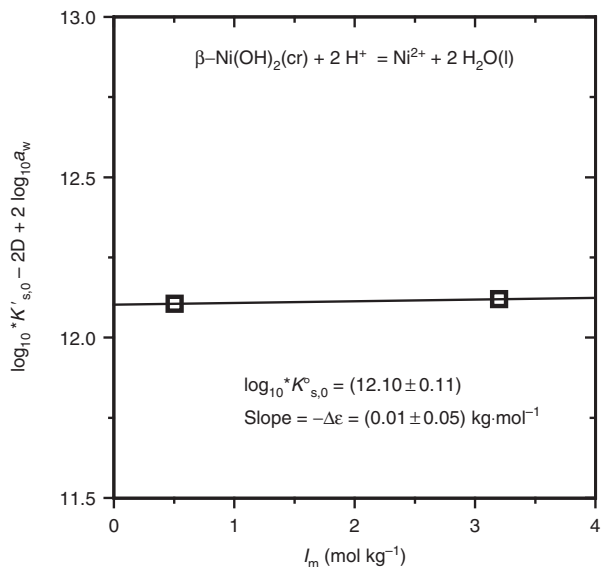


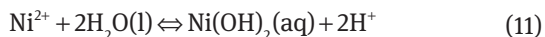
Figure 4: SIT-plot for the solubility reaction $\beta\text{-Ni(OH)}_2(\text{cr}) + 2\text{H}^+ \rightleftharpoons \text{Ni}^{2+} + 2\text{H}_2\text{O}(\text{l})$. The size of the symbols is representative of the uncertainty of the experimentally determined $\log_{10} *K'_{s,0}$ (± 0.09 , as 2σ).

($\log_{10} *K^{\circ}_{s,0} = (11.03 \pm 0.28)$). However, our value is not very different from the recent recommendation by Brown and Ekberg [18] for the microcrystalline phase ($\log_{10} *K^{\circ}_{s,0}\{\beta\text{-Ni(OH)}_2(\text{cr})\} = (11.75 \pm 0.13)$, see also Table 1). Minor discrepancies arising with the solubility product reported by Palmer and Gamsjäger [12] ($\log_{10} *K^{\circ}_{s,0} = (11.67 \pm 0.20)$) can be clearly attributed to differences in the crystallinity/particle size of the investigated solids. Hence, the greater crystallinity of the solid phase used in Palmer and Gamsjäger [12] is supported by the narrower peak widths in their XRD diffractograms compared to our study, and is full in line with the expected solid obtained under the hydrothermal conditions used by these authors in the synthesis of $\beta\text{-Ni(OH)}_2(\text{cr})$ (up to 140°C).

A conditional equilibrium constant for reaction (5) was calculated as the average of $\log_{10}[\text{Ni}]$ values determined within $10 \leq \text{pH}_m \leq 13$ in 0.5 M NaCl. Considering $\varepsilon(\text{Ni(OH)}_2(\text{aq}), \text{Na}^+/\text{Cl}^-) = 0$ (by definition in SIT), we find:

$$\log_{10} K'_{s,(1,2)} = \log_{10} K^{\circ}_{s,(1,2)} = -(7.6 \pm 0.4)$$

where uncertainty is calculated as 2σ . Combining $\log_{10} *K^{\circ}_{s,(1,2)}$ with $\log_{10} *K^{\circ}_{s,0}$ reported above, we obtain:



$$\log_{10} K^{\circ}_{(1,2)} = -(19.7 \pm 0.4)$$

This value is significantly greater than $\log_{10} *K^{\circ}_{(1,2)} = -21.15$ reported by Palmer and co-workers [30] and recommended in Brown and Ekberg [18]. These

authors derived $\log_{10} *K^{\circ}_{(1,2)}$ from solubility experiments with $\text{NiO}(\text{cr})$ in the temperature range $25\text{--}350^\circ\text{C}$ [27, 30]. The combination of this value with $\log_{10} *K^{\circ}_{s,0}$ selected in [18] for microcrystalline $\beta\text{-Ni(OH)}_2(\text{cr})$ results in $\log_{10} *K^{\circ}_{s,(1,2)} = -(9.40 \pm 0.14)$. The calculated solubility at $\text{pH}_m > 10$ obtained using these data is almost two orders of magnitude lower than our experimentally measured $\log_{10}[\text{Ni}]$ in this pH_m -region (see Figure 2). A close inspection of the original experimental data suggests that the value of $\log_{10} *K^{\circ}_{(1,2)}$ reported by Palmer et al. [30] and recommended in Brown and Ekberg [18] is possibly underestimated, very likely due to the inherent problems associated with the investigation of the solubility with a metastable phase (e.g. $\text{NiO}(\text{cr})$ at $T = 25^\circ\text{C}$)². Note that if assuming $\beta\text{-Ni(OH)}_2(\text{cr})$ as the solid phase controlling the solubility of Ni(II) at $T = 25^\circ\text{C}$ in [30], the combination of $\log_{10} *K^{\circ}_{s,(1,2)} = -(8.5 \pm 0.2)$ reported for this system (experimental value, table 3 in [30]) with $\log_{10} *K^{\circ}_{s,0}\{\beta\text{-Ni(OH)}_2(\text{cr})\} = (11.67 \pm 0.20)$ reported by the same authors in [12] results in $\log_{10} *K^{\circ}_{(1,2)} = -(20.17 \pm 0.30)$. This value agrees within the uncertainties with $\log_{10} *K^{\circ}_{(1,2)}$ determined in the present work. In a conference paper [29], the same authors reported experimental solubility data for $\text{NiO}(\text{cr})$ and $\beta\text{-Ni(OH)}_2(\text{cr})$ extending up to $\text{pH}_m = 13$, and determined at $T = 25^\circ\text{C}$ $\log_{10} *K^{\circ}_{s,0}\{\beta\text{-Ni(OH)}_2(\text{cr})\} = (11.6 \pm 0.2)$ (Figure 4 in [29]) and $\log_{10} *K^{\circ}_{s,(1,2)} = -(8.6 \pm 0.1)$ (Figure 5 in [29]). The combination of both solubility constants results in $\log_{10} *K^{\circ}_{(1,2)} = -(20.2 \pm 0.2)$, which again agrees within the uncertainties with $\log_{10} *K^{\circ}_{(1,2)}$ determined in the present study.

Solubility data collected in the present work clearly do not support the formation of the anionic hydrolysis species Ni(OH)_3^- . Experimental data shown in Figure 2 for 0.5 M NaCl–NaOH solutions with $10.0 \leq \text{pH}_m \leq 13.0$ indicate a constant $\log_{10}[\text{Ni}]_{\text{tot}} \approx -7.6$. The solubility data collected in 3.0 M NaCl–NaOH solutions with $10.0 \leq \text{pH}_m \leq 14.0$ are in all the cases below the detection limit of the technique for this salt concentration. These observations support the findings by Palmer and co-workers, and are in disagreement with the predominance of Ni(OH)_3^- species under hyperalkaline pH conditions as selected in the NEA–TDB [13] based on a single experimental solubility study [20].

² All experiments in Tremain and LeBlanc [27] were performed at 150 and 300°C . Palmer and Gamsjäger [12] reported that $\text{NiO}(\text{cr})$ is not stable below $T = 77^\circ\text{C}$. The same authors claimed that $\text{NiO}(\text{cr})$ remains metastable for a certain time at $T < 77^\circ\text{C}$, and thus that their experiments below this temperature with short equilibration times were representative of the equilibrium with $\text{NiO}(\text{cr})$. Although only two XRD diffractograms are provided in this publication, the authors acknowledge the possible presence of $\beta\text{-Ni(OH)}_2(\text{cr})$ in their sample at $T = 0.3^\circ\text{C}$ based on the small peak at $2\theta \approx 19^\circ$.

5 Experimental results in the presence of ISA

5.1 Solubility of Ni(II) in 0.5 M NaCl–NaOH–NaISA systems

The experimentally measured solubility of Ni(II) in the presence of [ISA] = 0.01, 0.1 and 0.2 M is shown in Figure 5. The figure includes thermodynamic calculations for the solubility of β -Ni(OH)₂(cr) in the absence and presence of ISA using thermodynamic data derived in the present work (details of the model in Section 5.3), as well as thermodynamic calculations in the presence of ISA based on the thermodynamic data selection in ThermoChimie [17]. Note that ThermoChimie considers $\log_{10}^* K_{s,0}^{\circ} \{\beta\text{-Ni(OH)}_2(\text{cr})\} = (11.03 \pm 0.28)$ as currently selected in the NEA–TDB [13]. This value is significantly lower than $\log_{10}^* K_{s,0}^{\circ} \{\beta\text{-Ni(OH)}_2(\text{cr})\}$ determined

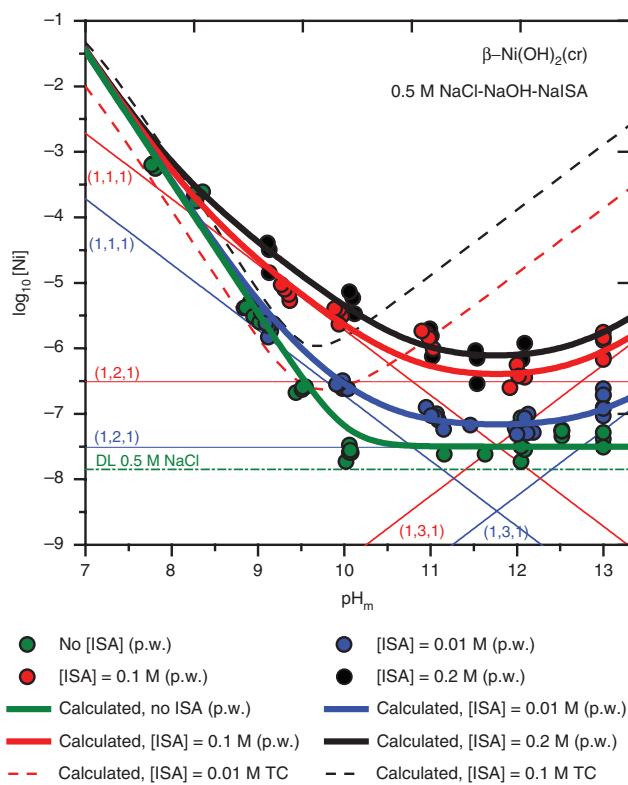


Figure 5: Experimental solubility data of Ni(II) determined in the present work in 0.5 M NaCl–NaOH solutions, in the absence and presence of NaISA (0.01, 0.1 and 0.2 M). Solid lines corresponding to the solubility of $\beta\text{-Ni(OH)}_2(\text{cr})$ (thick lines) and underlying aqueous speciation (thin lines) in the absence and presence of NaISA as calculated with the thermodynamic model derived in the present work. Dashed lines corresponding to the solubility of $\beta\text{-Ni(OH)}_2(\text{cr})$ as calculated with the current thermodynamic selection in ThermoChimie [17].

in the present work (see Section 4.3), and thus the calculated solubility (in the absence of ISA) is lower than [Ni] experimentally measured in the present work.

Experimental data in Figure 5 show a clear and steadily increase of Ni(II) solubility with increasing [ISA]. As the solubility limiting solid Ni(II) phase is the same in all investigated samples, this clearly indicates significant Ni(II)–ISA complexation. The increase in solubility is more evident above $\text{pH}_m \approx 10$, and becomes almost pH-independent at $\text{pH}_m \geq 11$. Below $\text{pH}_m \approx 10$, the impact of ISA on the solubility of Ni(II) becomes less relevant. In the case of [ISA] = 0.01 M, the solubility curve in the presence of ISA eventually merges with the solubility of Ni(II) in the absence of ISA at $\text{pH}_m \approx 9$. This observation reflects a distinct pH_m -dependency of the solubility of Ni(II) in the absence and presence of ISA within this pH_m -region, consequently involving a different number of H⁺ in the corresponding chemical reactions controlling the solubility in both systems.

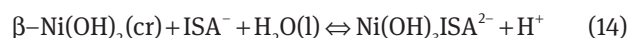
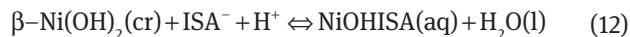
The increase in the solubility of Ni(II) with slope of +1 predicted by ThermoChimie [17] in the presence of ISA at $\text{pH}_m \geq 9.5$ (due to the formation of $\text{Ni(OH)}_3\text{ISA}^{2-}$) is not reproduced by experimental evidences obtained in the present work. A slight pH_m dependency can be claimed at pH_m values above 12.5, however, confirmed by the experimental data collected in our work up to $\text{pH}_m = 13$.

5.2 Solid phase characterization

The comparison of the XRD data collected for solubility experiments in the absence and presence of ISA shows that no solid phase alteration took place in the course of the experiments with ISA (Figure 6). The collected XRD patterns perfectly match those of $\beta\text{-Ni(OH)}_2(\text{cr})$ (PDF 73-1520), and thus the latter solid phase is considered to control the solubility of Ni(II) in the thermodynamic interpretation summarized in the following section.

5.3 Thermodynamic interpretation of Ni(II) solubility in the presence of NaISA

On the basis of slope analyses and solid phase characterization, chemical reactions (12)–(14) are proposed to be controlling the solubility of Ni(II) in the presence of ISA.



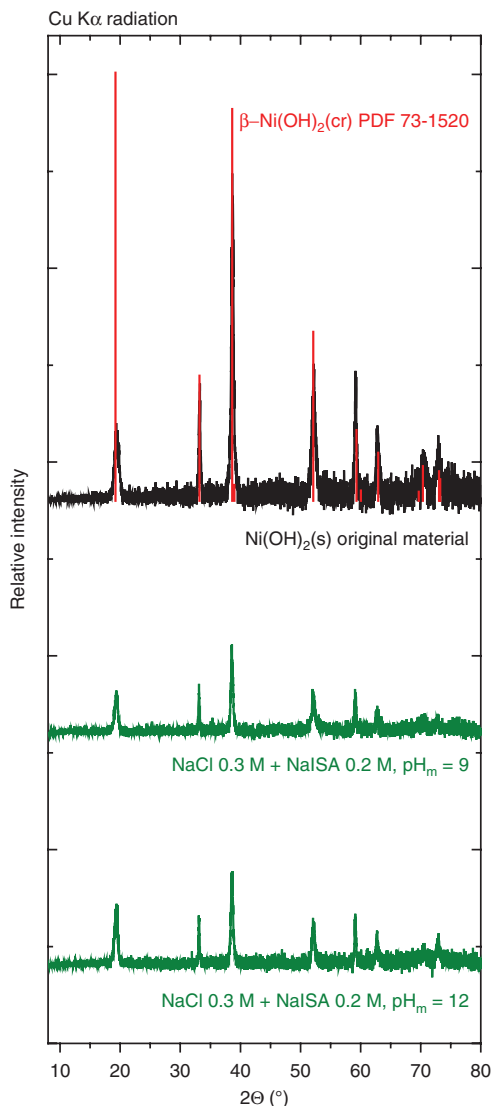


Figure 6: XRD spectra of selected solid phases from Ni(II) solubility experiments in 0.5 M NaCl–NaISA in the absence and presence of NaISA (0.2 M). Red marks indicate peak positions for β -Ni(OH)₂(cr) reference spectrum (PDF 73-1520).

with

$$\log_{10} {}^*K'_{s,(1,1,1)} = \log_{10}[\text{NiOHISA}(\text{aq})] - \log_{10}[\text{ISA}^-] - \log_{10}[\text{H}^+]$$

$$\log_{10} {}^*K'_{s,(1,2,1)} = \log_{10}[\text{Ni}(\text{OH})_2\text{ISA}^-] - \log_{10}[\text{ISA}^-]$$

$$\log_{10} {}^*K'_{s,(1,3,1)} = \log_{10}[\text{Ni}(\text{OH})_3\text{ISA}^{2-}] + \log_{10}[\text{H}^+] - \log_{10}[\text{ISA}^-]$$

The fit of Ni(II) solubility data in the presence of $[\text{ISA}] = 0.01, 0.1$ and 0.2 M, in combination with the chemical model proposed above, results in a consistent set of conditional solubility constants satisfactorily explaining all experimental data collected in this work. Uncertainties reported for the corresponding $\log_{10} {}^*K'_{s,(1,n,1)}$ values are calculated as 2σ .

$$\log_{10} {}^*K'_{s,(1,1,1)}(I = 0.5 \text{ M NaCl}) = (5.3 \pm 0.3)$$

$$\log_{10} {}^*K'_{s,(1,2,1)}(I = 0.5 \text{ M NaCl}) = -(5.5 \pm 0.5)$$

$$\log_{10} {}^*K'_{s,(1,3,1)}(I = 0.5 \text{ M NaCl}) = -(18.3 \pm 0.7)$$

The experimental solubility data were also analysed deliberately including the species NiISA⁺ in the fit. This attempt was not converging, because Ni(II) solubility within $8 \leq \text{pH}_m \leq 10$ has an obviously different dependency on pH_m in the absence (slope $\{\log_{10}[\text{Ni}] \text{ vs. } \text{pH}_m\} \approx -2$, predominance of Ni²⁺ in solution) and presence (slope $\{\log_{10}[\text{Ni}] \text{ vs. } \text{pH}_m\} \approx -1$, predominance of NiOHISA(aq) in solution) of ISA. Warwick et al. [32] and Almond et al. [33] proposed $2.1 \leq \log_{10} {}^*K' \leq 2.6$ for the equilibrium reaction $\text{Ni}^{2+} + \text{ISA}^- \rightleftharpoons \text{NiISA}^+$, based on polarographic and potentiometric measurements at $\text{pH} \approx 7$. Although our experimental data do not allow to either confirm or disregard the formation of NiISA⁺ at $\text{pH} \approx 7$, we can safely claim that the impact of this species on the solubility of β -Ni(OH)₂(cr) is rather minor, and that the stability constants reported by Warwick et al. [32] and Almond et al. [33] are probably overestimated.

The predominance of the species NiOHISA(aq) in the pH_m -range 8–10 provides indirect information on the structure of the Ni(II)–ISA complex forming. For the same pH_m -range but in the absence of ISA, the species Ni²⁺ has been shown to prevail in solution. It appears evident that the complexation of Ni²⁺ with ISA⁻ (thus with a strong electron-donor) cannot enhance the acidity of the Ni²⁺ cation and promote its hydrolysis, otherwise absent (for this pH_m -range) in ISA-free solutions. Instead, as discussed in Section 3.5, the complexation of Ni²⁺ with ISA⁻ is expected to enhance the acidity of the α -OH group of the ligand, which is deprotonated above $-\log_{10}[\text{H}^+] \approx 8$: the complex forming is very likely NiISA_H(aq). Note that in the absence of any (hard-Lewis) metal cation, the deprotonation of the α -OH group of ISA has been estimated to take place at $-\log_{10}[\text{H}^+] \approx 14.3$ [35].

The Ni(II)–ISA species forming at $\text{pH}_m \geq 12.5$ has been formulated as Ni(OH)₃ISA²⁻. However, this formulation is also unlikely considering the aqueous speciation of Ni(II) in the absence of ISA, where the formation of the anionic species Ni(OH)₃⁻ has not been observed within the investigated pH_m -range. Thus, a structure invoking the deprotonation of the α -OH group of ISA, Ni(OH)₂ISA_H²⁻, appears again more likely. In the absence of definitive spectroscopic proof for the proposed hypotheses, we have maintained the nomenclature of Ni(II)–ISA complexes involving only the hydrolysis of Ni(II), Ni(OH)_xISA^{1-x} (with $x = 1-3$).

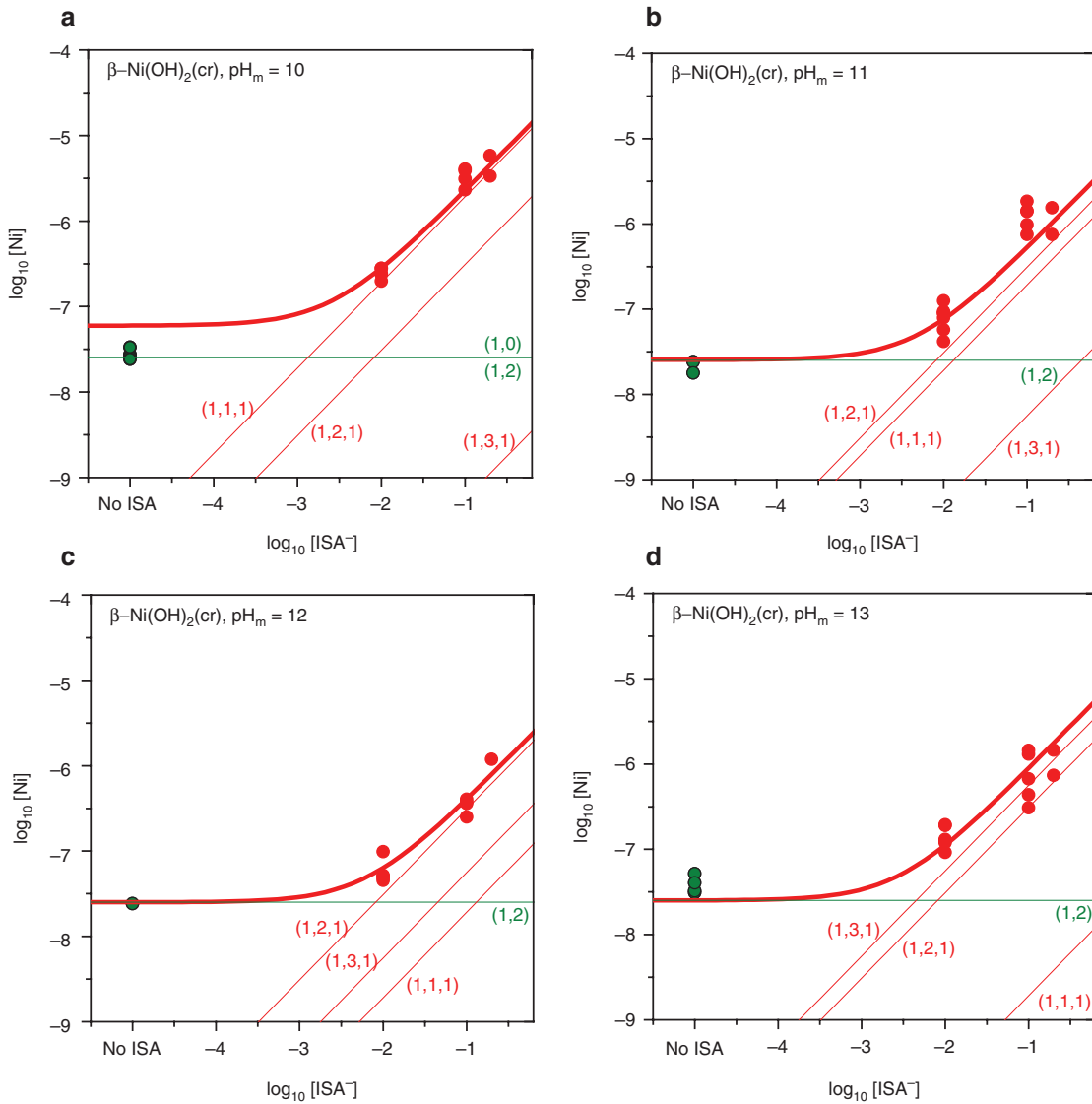


Figure 7: Experimental Ni(II) solubility data determined in the present work in 0.5 M NaCl–NaOH at increasing NaISA concentrations (0.01, 0.1 and 0.2 M; red symbols). Solubility data determined for the same pH_m in the absence of ISA are included (green symbols) for comparison. Solid lines corresponding to the overall solubility of $\beta\text{-Ni(OH)}_2(\text{cr})$ calculated with the thermodynamic model derived in the present work (thick lines) and underlying aqueous speciation (thin lines).

Experiments in the presence of NaISA have been conducted at $I=0.5$ M NaCl–NaOH, and thus the extrapolation to $I=0$ has been done by using the following SIT ion interaction coefficients:

- $\varepsilon(\text{ISA}^-, \text{Na}^+) = -(0.07 \pm 0.01) \text{ kg} \cdot \text{mol}^{-1}$ (in analogy to Hox^- , as proposed in [47])
- $\varepsilon(\text{NiOHISA}(\text{aq}), \text{Na}^+/\text{Cl}^-) = 0$ [by definition in SIT]
- $\varepsilon(\text{Ni(OH)}_2\text{ISA}^-, \text{Na}^+) = -(0.05 \pm 0.10) \text{ kg} \cdot \text{mol}^{-1}$ [estimated by charge analogy] [49]
- $\varepsilon(\text{Ni(OH)}_3\text{ISA}^{2-}, \text{Na}^+) = -(0.10 \pm 0.10) \text{ kg} \cdot \text{mol}^{-1}$ [estimated by charge analogy] [49]

and

$$\log_{10} {}^*K_{s,(1,1,1)}^{\circ} = \log_{10} {}^*K'_{s,(1,1,1)} + \log_{10} \gamma_{\text{NiOHISA}(\text{aq})} + \log_{10} a_w - \log_{10} \gamma_{\text{ISA}^-} - \log_{10} \gamma_{\text{H}^+}$$

$$\log_{10} {}^*K_{s,(1,2,1)}^{\circ} = \log_{10} {}^*K'_{s,(1,2,1)} + \log_{10} \gamma_{\text{Ni(OH)}_2\text{ISA}^-} - \log_{10} \gamma_{\text{ISA}^-}$$

$$\log_{10} {}^*K_{s,(1,3,1)}^{\circ} = \log_{10} {}^*K'_{s,(1,3,1)} + \log_{10} \gamma_{\text{Ni(OH)}_3\text{ISA}^{2-}} + \log_{10} \gamma_{\text{H}^+} - \log_{10} \gamma_{\text{ISA}^-} - \log_{10} a_w$$

resulting in:

$$\log_{10} {}^*K_{s,(1,1,1)}^{\circ} = (5.6 \pm 0.3)$$

$$\log_{10} {}^*K_{s,(1,2,1)}^{\circ} = -(5.5 \pm 0.5)$$

Table 3: Stability constants for the solubility, hydroxide and ISA complexes of Ni(II) as derived in the present work (p.w.) or reported in Gamsjäger et al. [13].

		Reference
Solubility	$\log_{10} *K_{s,0}^{\circ}$	
$\beta\text{-Ni(OH)}_2(\text{cr}) + 2 \text{H}^+ \Leftrightarrow \text{Ni}^{2+} + 2 \text{H}_2\text{O}(\text{l})$	(12.10 ± 0.11)	(p.w.)
Hydroxide complexes	$\log_{10} *K_{(1,n)}^{\circ}$	
$\text{Ni}^{2+} + 2 \text{H}_2\text{O}(\text{l}) \Leftrightarrow \text{Ni(OH)}_2(\text{aq}) + 2 \text{H}^+$	$-(19.7 \pm 0.4)$	(p.w.)
Chloride complexes	$\log_{10} K_{(1,n)}^{\circ}$	
$\text{Ni}^{2+} + \text{Cl}^- \Leftrightarrow \text{NiCl}^+$	(0.08 ± 0.60)	Gamsjäger et al. [13]
ISA complexes	$\log_{10} *K_{(1,n,1)}^{\circ}$	
$\text{Ni}^{2+} + \text{H}_2\text{O}(\text{l}) + \text{ISA}^- \Leftrightarrow \text{NiOHISA}(\text{aq}) + \text{H}^+$	$-(6.5 \pm 0.3)$	(p.w.)
$\text{Ni}^{2+} + 2 \text{H}_2\text{O}(\text{l}) + \text{ISA}^- \Leftrightarrow \text{Ni(OH)}_2\text{ISA}^- + 2 \text{H}^+$	$-(17.6 \pm 0.5)$	(p.w.)
$\text{Ni}^{2+} + 3 \text{H}_2\text{O}(\text{l}) + \text{ISA}^- \Leftrightarrow \text{Ni(OH)}_3\text{ISA}^{2-} + 3 \text{H}^+$	$-(31.0 \pm 0.7)$	(p.w.)

$$\log_{10} *K_{s,(1,3,1)}^{\circ} = -(18.9 \pm 0.7)$$

The combination of $\log_{10} *K_{s,(1,n,1)}^{\circ}$ ($n=1-3$) with $\log_{10} *K_{s,0}^{\circ}\{\beta\text{-Ni(OH)}_2(\text{cr})\}$ determined in Section 4.3, allows the calculation of the equilibrium constants for the formation of the complexes NiOHISA(aq), Ni(OH)₂ISA⁻ and Ni(OH)₃ISA²⁻ as summarized in Table 3.

The comparison of thermodynamic calculations using the model derived in the present work with experimental solubility data is provided in Figure 5 (as a function of pH_m), and further in Figure 7 as a function of $\log_{10}[\text{ISA}]$. A good agreement is obtained between the experimental and calculated Ni(II)-solubilities for all investigated systems, thus supporting the chemical and thermodynamic models derived for Ni(II) in the presence of ISA.

5.4 Chemical, thermodynamic and activity models for the system $\text{Ni}^{2+}\text{-Na}^+\text{-H}^+\text{-Cl}^-\text{-OH}^-\text{-ISA}^-\text{-H}_2\text{O}(\text{l})$

Table 3 summarizes the chemical and thermodynamic models derived in the present work or reported in

Gamsjäger et al. [13] for Ni(II) in the absence and presence of ISA⁻. These models properly explain experimental solubility data collected at $8 \leq \text{pH}_m \leq 13$. Table 4 provides all SIT ion interaction coefficients used in the present work and involving Ni(II), either as reported in Gamsjäger et al. [13] or estimated in the present work.

6 Conclusions

The solubility of Ni(II) in dilute to concentrated aqueous NaCl–NaOH systems ($I \leq 3.0$ M) in the absence of ISA is controlled by $\beta\text{-Ni(OH)}_2(\text{cr})$, and can be explained by the predominance of Ni²⁺ and Ni(OH)₂(aq) in the aqueous phase. Differences in $\log_{10} *K_{s,0}^{\circ}\{\beta\text{-Ni(OH)}_2(\text{cr})\}$ determined in the present work and the data available in the literature highlight the important role of particle size/crystallinity effects in the solubility-control of this system. The use of $\log_{10} *K_{s,0}^{\circ}\{\beta\text{-Ni(OH)}_2(\text{cr})\}$ currently selected in the NEA–TDB [13] for a very crystalline solid phase tends to underestimate the solubility of Ni(II) in natural and anthropogenic systems. We found no evidence for the formation of the anionic species Ni(OH)₃⁻ up to $\text{pH}_m \leq 13$. The solubility of $\beta\text{-Ni(OH)}_2(\text{cr})$ remains pH_m -independent with total nickel concentration below $\approx 10^{-7}$ M within the pH_m range 10 to 13.

The solubility of Ni(II) at $7.5 \leq \text{pH}_m \leq 13$ is increased up to two orders of magnitude in the presence of ISA relative to comparable ISA-free systems. These results confirm the capacity of ISA to outcompete hydrolysis even under strongly alkaline pH_m conditions. Solubility data determined in the present work can be properly explained with a simple chemical model including the predominance of the complexes NiOHISA(aq), Ni(OH)₂ISA⁻ and Ni(OH)₃ISA²⁻ in the aqueous phase. These results furthermore provide indirect evidence on the deprotonation of the $\alpha\text{-OH}$ group of ISA at $\text{pH}_m > 8$ induced by the complexation with Ni(II).

This work represents the most comprehensive experimental study available to date reporting chemical,

Table 4: SIT ion interaction coefficients used in the present work for Ni(II) hydroxide and ISA complexes.

<i>i</i>	<i>j</i>	$\epsilon(i, j)$	References
Ni ²⁺	Cl ⁻	(0.17 ± 0.02)	Gamsjäger et al. [13]
NiCl ⁺	Cl ⁻	(0.21 ± 0.06)	Estimated by correlation with $\epsilon(i, \text{ClO}_4^-)$
Ni(OH) ₂ (aq)	Na ⁺ /Cl ⁻	0	By definition in SIT
NiOHISA(aq)	Na ⁺ /Cl ⁻	0	By definition in SIT
Ni(OH) ₂ ISA ⁻	Na ⁺	$-(0.05 \pm 0.10)$	Estimated by charge analogy [49]
Ni(OH) ₃ ISA ²⁻	Na ⁺	$-(0.10 \pm 0.10)$	Estimated by charge analogy [49]

thermodynamic and activity models for the system $\text{Ni}^{2+}\text{-Na}^+\text{-H}^+\text{-Cl}^-\text{-OH}^-\text{-ISA}^-\text{-H}_2\text{O(l)}$ at low to intermediate ionic strength, valid from near-neutral to hyperalkaline pH_m conditions. The equilibrium models developed represent a significant improvement and are highly relevant for calculating reliable Ni(II) source term concentrations in the context of safety assessments for L/ILW repositories.

Acknowledgements: The research leading to this study was funded by SKB. Klas Källström (SKB) and Mireia Grivé (Amphos²¹) are kindly acknowledged for their stimulating scientific discussions. The contribution of Melanie Böttle, Agost Tasi, Björn Beele and Christian Adam (KIT-INE) in the synthesis and characterization of $\text{Ca(ISA)}_2(\text{s})$ and $\text{NaISA}(\text{s})$ is highly appreciated. Frank Geyer and Annika Kaufmann (KIT-INE) are gratefully acknowledged for the ICP-MS measurements.

References

- Duro, L., Domènech, C., Grivé, M., Roman-Ross, G., Bruno, J., Källström, K.: Assessment of the evolution of the redox conditions in a low and intermediate level nuclear waste repository (SFR1, Sweden). *Appl. Geochem.* **49**, 192 (2014).
- Lindgren, M., Pettersson, M., Wiborgh, M.: Correlation factors for C-14, Cl-36, Ni-59, Ni-63, Mo-93, Tc-99, I-129 and Cs-135 in operational waste for SFR1, Svensk Kärnbränslehantering AB, Stockholm (2007).
- SKB, Safety analysis for SFR Long-term safety, Main report for the safety assessment SR-PSU, Svensk Kärnbränslehantering AB, Stockholm (2015).
- Almkvist, L., Gordon, A.: Low and intermediate level Reference waste inventory 2007, Svensk Kärnbränslehantering AB, Stockholm (2007).
- Fanger, G., Skagius, K., Wiborgh, M.: Complexing agents in SFR, Svensk Kärnbränslehantering AB, Stockholm (2001).
- Grivé, M., Colàs, E., García, D., González-Siso, M. R., Duro, L., Bruno, J.: Influence of organic ligands on the solubility and sorption of radionuclides in cement environments: an easy-to-handle tool for PA, At Het Pand, Ghent, Belgium (2013).
- Bradbury, M. H., Van Loon, L. R.: Cementitious Near-field Sorption Data Bases for Performance Assessment of a L/ILW Repository in a Palfris Host Rock, PSI Bericht 98-01, CEM-94: Update I (1997).
- Van Loon, L. R., Glaus, M. A.: Review of the kinetics of alkaline degradation Of cellulose in view of its relevance for safety assessment of radioactive waste repositories. *J. Environ. Polym. Degrad.* **5**, 97 (1997).
- Van Loon, L. R., Glaus, M. A.: Experimental and theoretical studies on alkaline degradation of cellulose and its impact on the sorption of radionuclides, Nagra TR 97-04 (1998).
- Glaus, M. A., Van Loon, L. R.: Degradation of cellulose under alkaline conditions: new insights from a 12 years degradation study. *J. Environ. Polym. Degrad.* **42**, 2906 (2008).
- Glaus, M. A., Van Loon, L. R., Schwyn, B., Vines, S., Williams, S. J., Larsson, P., Puigdomenech, I.: Long-term predictions of the concentration of α -isosccharinic acid in cement pore water. *Mater. Res. Soc. Symp. Proc.* **1107**, 605 (2008).
- Palmer, D. A., Gamsjäger, H.: Solubility measurements of crystalline $\beta\text{-Ni(OH)}_2$ in aqueous solution as a function of temperature and pH. *J. Coord. Chem.* **63**, 2888 (2010).
- Gamsjäger, H., Bugajski, J., Gajda, T., Lemire, R. J., Preis, W.: Chemical thermodynamics of Nickel. (OECD, NEA-TDB) Elsevier, Science Publishers B.V., Amsterdam (2005).
- Schindler, P. W.: Heterogeneous equilibria involving oxides, hydroxides, carbonates and hydroxide carbonates. In equilibrium concepts in natural water systems. *Adv. Chem. Ser.* **67**, 196 (1967).
- Bruno, J.: A Reinterpretation of the solubility product of solid uranium(IV) dioxide. *Acta Chem. Scand.* **43**, 99 (1989).
- Neck, V., Altmaier, M., Seibert, A., Yun, J. L., Marquardt, C. M., Fanghänel, Th.: Solubility and redox reactions of Pu(IV) hydrous oxide: Evidence for the formation of $\text{PuO}_{2+x}(\text{s, hyd})$. *Radiochim. Acta.* **95**, 193 (2007).
- Giffaut, E., Grivé, M., Blanc, P., Vieillard, Ph., Colàs, E., Gailhanou, H., Gaboreau, H., Gaboreau, S., Marty, N., Madé, B., Duro, L.: Andra thermodynamic database for performance assessment: ThermoChimie. *Appl. Geochem.* **49**, 225 (2014).
- Brown, P. L., Ekberg, C.: Hydrolysis of Metal Ions. Wiley-VCH Verlag GmbH & Co., Germany (2016).
- Britton, H. T. S.: Electrometric studies of the precipitation of hydroxides. Part I. Precipitation of magnesium, manganous, ferrous, cobalt, nickel and thorium hydroxides by use of the hydrogen electrode. *J. Chem. Soc.* **127**, 2110 (1925).
- Gayer, K. H., Garret, A. B.: The equilibria of nickel hydroxide, Ni(OH)_2 , in solutions of hydrochloric acid and sodium hydroxide at 25°C. *J. Am. Chem. Soc.* **71**, 2973 (1949).
- Feitknecht, W., Hartmann, L.: Die Löslichkeitsprodukte von nickel- und kobalthydroxyden. *Chimia.* **8**, 95 (1954).
- Novak-Adamic, D. M., Cosovic, B., Bilinski, H., Branica, M.: Precipitation and hydrolysis of metallic ions—V: Nickel(II) in aqueous solutions. *J. Inorg. Nucl. Chem.* **35**, 2371 (1973).
- Poulson, S. R., Drever, J. I.: Aqueous complexing of nickel and zinc with 3-(N-morpholino) propanesulfonic acid and the solubility products of nickel and zinc hydroxides. *Talanta* **43**, 1975 (1996).
- Mattigod, S. V., Rai, D., Felmy, A. R., Rao, L.: Solubility and solubility product of crystalline Ni(OH)_2 . *J. Solution. Chem.* **26**, 391 (1997).
- Plyasunova, N. V., Zhang, Y., Mohammed, M.: Critical evaluation of thermodynamics of complex formation of metal ions in solutions. IV. Hydrolysis and hydroxo-complexes of Ni^{2+} at 298.15 K. *Hydrometallurgy*, **48**, 43 (1998).
- Ziemniak, S. E., Goyette, M. A.: Nickel(II) Oxide Solubility and Phase Stability in high temperature Aqueous solutions. *J. Sol Chem.* **33**, 1135 (2004).
- Tremaine, P. R., Leblanc, J. C.: The solubility of nickel oxide and hydrolysis of Ni^{2+} in water to 573 K. *J. Chem. Thermodyn.* **12**, 521 (1980).
- Ziemniak, S. E., Jones, M. E., Combs, K. E. S.: Solubility and phase behavior of nickel oxide in aqueous sodium phosphate solutions at elevated temperatures. *J. Sol Chem.* **18**, 1133 (1989).

29. Palmer, D. A., Bénézeth, P., Wesolowski, D. J.: Solubility of Nickel Oxide and Hydroxide in Water. 14th Int. Conf. Prop. Water Steam Kyoto (2004).
30. Palmer, D. A., Bénézeth, P., Xiao, C., Wesolowski, D. J., Anovitz, L. M.: Solubility measurements of crystalline NiO in aqueous solution as a function of temperature and pH. *J. Sol Chem.* **40**, 680 (2011).
31. Felipe-Sotelo, M., Hinchliff, J., Field, L. P., Milodowski, A. E., Holt, J. D., Taylor, S. E., Read, D.: The solubility of nickel and its migration through the cementitious backfill of a geological disposal facility for nuclear waste. *J. Hazard Mater.* **15**, 314, 211 (2016).
32. Warwick, P., Evans, N., Hall, T., Vines, S.: Complexation of Ni(II) by α -isosaccharinic acid and gluconic acid from pH 7 to pH 13. *Radiochim. Acta.* **91**, 233–240 (2003).
33. Almond, M., Belton, D., Humphreys, P. N., Laws, A. P.: A study of the metal binding capacity of saccharinic acids formed during the alkali catalysed decomposition of cellulosic materials: nickel complexation by glucoisosaccharinic acids and xyloisosaccharinic acids. *Carbohydr. Res.* **427**, 48–54 (2016).
34. Motellier, S., Charles, Y.: Characterization of acid–base and complexation properties of cellulose degradation products using capillary electrophoresis. *Anal. Chim. Acta.* **375**(3), 243 (1998).
35. Evans, N.: Studies on Metal α -Isosaccharinic Acid Complexes. PhD thesis, Loughborough University (2003).
36. Whistler, R., BeMiller, J.: *Methods in Carbohydrate Chemistry*, Vol. 2, Reactions of Carbohydrates, Academic Press, New York (1961).
37. Vercammen, K.: Complexation of Calcium, Thorium and Europium by alpha-Isosaccharinic Acid under Alkaline Conditions. PhD thesis, Swiss Federal Institute of Technology Zurich (2000).
38. Greenfield, B. J., Harrison, W. N., Robertson, G. P., Somers, P. J., Spindler, M.W.: *Mechanistic Studies of the Alkaline Degradation of Cellulose in Cement*, AEA Technology Plc, Harwell, UK (1993).
39. Glaus, M. A., Van Loon, L. R., Achatz, S., Chodura, A., Fischer, K.: Degradation of cellulosic materials under the alkaline conditions of acementitious repository for low and intermediate level radioactive waste Part I: Identification of degradation products. *Anal. Chim. Acta.* **398**, 111 (1999).
40. Pointeau, I., Hainos, D., Coreau, N., Reiller, P.: Effect of organics on selenite uptake by cementitious materials. *Waste Manag.* **26**, 733 (2006).
41. Colàs, E.: Complexation of Th(IV) and U(VI) by polyhydroxy and polyamino carboxylic acids. PhD thesis, Universitat Politècnica de Catalunya (UPC) (2013).
42. Rai, D., Rao, L., Moore, A.: The influence of isosaccharinic acid on the solubility of Np(IV) hydrous oxide. *Radiochim. Acta.* **83**, 9 (1998).
43. Altmaier, M., Metz, V., Neck, V., Muller, R., Fanghänel, T.: Solid-liquid equilibria of $\text{Mg}(\text{OH})_2(\text{cr})$ and $\text{Mg}_2(\text{OH})_3\text{Cl}\cdot 4\text{H}_2\text{O}(\text{cr})$ in the system Mg-Na-H-OH-O-Cl-H₂O at 25°C. *Geochim. Cosmochim. Acta.* **67**, 3595 (2003).
44. Herm, M., Gaona, X., Rabung, Th., Fellhauer, D., Crepin, C., Dardenne, K., Altmaier, M., Geckeis, H.: Solubility and spectroscopic study of AnIII/LnIII in dilute to concentrated Na–Mg–Ca–Cl–NO₃ solutions. *Pure and Applied Chem.* **87**(5), 487 (2015).
45. Guillaumont, R., Fanghänel, T., Fuger, J., Grenthe, I., Neck, V., Palmer, D.A., Rand, M.H.: Update on the chemical thermodynamics of U, Np, Pu, Am and Tc. (OECD, NEA-TDB) Elsevier, Science Publishers B. V., Amsterdam (2003).
46. Ciavatta, L.: The specific interaction theory in evaluating ionic equilibria. *Annali Di Chimica.* **70**, 551 (1980).
47. Hummel, W., Anderegg, G., Rao, L., Puigdomènech, I., Tochiyama, O.: *Chemical Thermodynamics of Compounds and Complexes of U, Np, Pu, Am, Tc, Se, Ni and Zr with Selected Organic Ligands.* (OECD, NEA-TDB) Elsevier, Science Publishers B. V., Amsterdam (2005).
48. Wanner, H., Östhols, E.: TDB3 Guidelines for the assignment of uncertainties. (OECD, NEA-TDB) Issy-les-Moulineaux, France (1999).
49. Hummel, W.: Ionic strength corrections and estimation of SIT ion interaction coefficients, Paul Scherrer Institut, PSI report TM-44-09-01 (2009).